AIAA 81-4124

The Variable-Speed Tail-Chase Aerial Combat Problem

B.S.A. Järmark*
SAAB-SCANIA AB, Linköping, Sweden
A.W. Merz†
Analytical Mechanics Associates, Inc., Mountain View, Calif.
and
J.V. Breakwell‡
Stanford University, Stanford, Calif.

The differential-game version of the coplanar tail-chase aerial combat problem is analyzed by the numerical differential dynamic programming method. The faster pursuer and the more maneuverable evader have only their turn rates as input controls, but their speeds fall as their turn rates are increased to the specified normal acceleration limit. The turn rate of the pursuer is such as to minimize the final miss-distance, while the evader's control maximizes this quantity. Solutions to the fifth-order problem are given for a range of flight conditions. Optimal control variations and sensitivities are discussed with respect to the conflicting requirements of high turn rates and high speed, which cannot be exploited simultaneously.

Introduction

THE differential-game version of the two-aircraft aerial combat problem has been studied under various assumptions with regard to the dynamic models and to role specification. Virtually all of the published material deals with very-low-order constant-speed dynamic models.[1-5] and only a few papers treat the roles of pursuer and evader as functions of the relative geometry and the weapon systems.[6,7] In the present case, the roles are fixed, and the initial geometry is specialized to that of a collinear tail chase. The minimum final range is then to be minimized by the faster pursuer and maximized by the more maneuverable evader.

An important difference in the dynamic model used is that the longitudinal acceleration of each aircraft depends on both the speed and the horizontal turn rate of the aircraft; thus, a high turn rate reduces the airspeed. Secondly, a structural limit on normal acceleration permits a higher turn rate only at a lower air speed. It is assumed that the thrust does not vary with the speed, and that the aircraft maneuver at constant altitude, so the motion is coplanar. While the equations thus remain relatively simple, solutions must be obtained numerically because the speeds and turn rates both vary with time during the maneuver.

The performance criterion in the maneuver optimization process is the miss-distance or minimum range. Although the evader's top speed is less than the pursuer's, the evader's maximum turn rate is higher. This means that the pursuer cannot follow the evader's maximum turn-rate trajectory, and therefore the miss-distance is always positive. The pursuer is to maneuver in order to minimize, and the evader in order to maximize this quantity, the turns being functions of the states which are the relative position and heading and the aircraft speeds. As implied by the "min-max" optimization condition, if only the evader deviates from his optimal control, the final miss-distance is reduced, while if only the pursuer's control is suboptimal, the miss-distance is increased, relative to the optimal value.

Received Jan. 14, 1980; revision received July 22, 1980.

*Research Scientist. Member AIAA.
†Senior Analyst; currently, Research Scientist, Lockheed Research Labs., Palo Alto, Calif. Associate Fellow AIAA.
‡Professor, Dept. of Aeronautics and Astronautics. Fellow AIAA.

Dynamic Equations

The coplanar motion of the two aircraft is modeled by the solution to the kinematic equations, giving the location (x,y) of the evading second aircraft (E) with respect to the pursuing first aircraft (P), in a nonrotating axis system fixed to aircraft 1. As shown in Fig. 1, the relative velocity has components

$$\dot{x} = v_2 \cos H_2 - v_1 \cos H_1 \tag{1}$$

$$\dot{y} = v_2 \sin H_2 - v_1 \sin H_1 \tag{2}$$

where the headings and speeds of both aircraft depend on the turn-rate controls input by the pilots:

$$\dot{H}_1 = -\omega_1 \qquad \dot{H}_2 = -\omega_2 \tag{3}$$

$$\dot{v}_1 = g\{A_1 - B_1 v_1^2 - C_1[(\omega_1/g)^2 + v_1^{-2}]\} \tag{4}$$

$$\dot{v}_2 = g\{A_2 - B_2 v_2^2 - C_2[(\omega_2/g)^2 + v_2^{-2}]\} \tag{5}$$

The last pair of equations can be derived by writing the longitudinal accelerations for low angles of attack; i.e.,

$$\dot{v} = (g/W)(T - D) \tag{6}$$

The drag is expressible as the sum of "zero-lift" component and an "induced" component, which is proportional to the

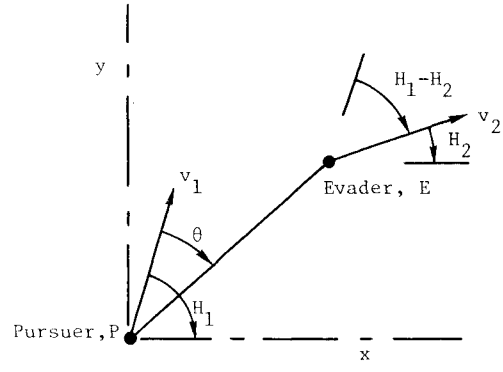

Fig. 1 Axis systems and relative geometry.

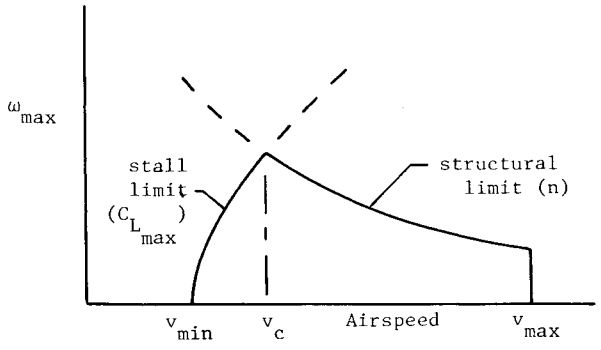

Fig. 2 Maximum turn-rate variation with velocity at constant altitude.

square of the lift coefficient

$$D=\tfrac{1}{2}\rho S v^2(C_{D_0}+k_D C_L^2) \tag{7}$$

Here the lift coefficient needed for a bank angle ϕ is

$$C_L=L/\tfrac{1}{2}\rho S v^2 \tag{8}$$

where $L\cos\phi=W$ and $L\sin\phi=Wv\omega/g$, so that

$$C_L=\frac{2W}{\rho S v}\left[\left(\frac{\omega}{g}\right)^2+v^{-2}\right]^{\frac{1}{2}} \tag{9}$$

therefore,

$$\frac{D}{W}=\frac{C_{D_0}\rho S}{2W}v^2+\frac{2Wk_D}{\rho S}\left[\left(\frac{\omega}{g}\right)^2+v^{-2}\right] \tag{10}$$

The constant coefficients in Eq. (4) can then be identified as

$$A_1=T/W \qquad B_1=SC_{D_0}/2W \qquad C_1=2Wk_D/\rho S \tag{11}$$

where the thrust, weight, and other parameters are those of aircraft 1. An analogous set of equations applies to aircraft 2 and to its coefficients A_2, B_2, and C_2.

The maximum load factor of each aircraft is constrained by the maximum lift coefficient at low speeds and by structural limits at high speeds. This means that the maximum turn rate varies with velocity as shown in Fig. 2. In this figure, v_c is the so-called "corner velocity" of the aircraft, at which the horizontal turn rate is a maximum. Whether this turn rate can be sustained depends upon the aircraft drag and the engine capability at this airspeed.

Optimization Problem§

The pursuer and evader are to optimize the "miss-distance," following from the tail-chase initial condition, by suitable choice of their turn directions and turn rates; i.e., the performance criterion is

$$J=\min_{\omega_1}\max_{\omega_2} r_f$$

Included in this optimization process is the evader's choice of initial range, at which both turn maneuvers begin.

The final time t_f occurs at minimum range, when the radial velocities are equal.

$$\dot r(t_f)=v_2\cos(H_1-H_2-\theta)-v_1\cos\theta=0 \tag{12}$$

The Hamiltonian corresponding to the dynamic equations is

$$\mathcal{H}=V_x\dot x+V_y\dot y+V_{H_1}\dot H_1+V_{H_2}\dot H_2+V_{v_1}\dot v_1+V_{v_2}\dot v_2 \tag{13}$$

where the adjoint vector V must satisfy $\dot V=-\partial\mathcal{H}/\partial x$, or

$$\dot V_x=0 \qquad \dot V_y=0 \tag{14}$$

$$\dot V_{H_1}=-v_1\sin H_1 \qquad \dot V_{H_2}=v_2\sin H_2 \tag{15}$$

$$\dot V_{v_1}=\cos H_1+2g(B_1v_1-C_1/v_1^3)V_{v_1} \tag{16}$$

$$\dot V_{v_2}=-\cos H_2+2g(B_2v_2-C_2/v_2^3)V_{v_2} \tag{17}$$

The velocity adjoint equations (16) and (17) must be modified if either turn rate takes its maximum value $\omega_{\max}(v)$. In this case,

$$\dot V_v=-\partial\mathcal{H}/\partial v-[\partial\mathcal{H}/\partial\omega]_{\omega_{\max}}\partial\omega_{\max}/\partial v \tag{18}$$

The payoff function is the terminal miss-distance. This implies that (V_x,V_y) at the final time t_f is a unit vector parallel to the relative position vector of E, and that the remaining adjoints vanish at t_f. But, according to Eqs. (14), V_x and V_y remain constant.

Suppose now that the reference x direction is chosen normal to the initial relative position vector. Since E is also optimizing the range (y_0) at which he initiates his turn to right or left, the initial value of V_y is zero. Hence (V_x,V_y) remains equal to (1,0) and, therefore, the final range vector is normal to the initial range vector; i.e., $H_1(t_f)=\theta(t_f)$.

The optimal turn-rate controls of the pursuing and evading aircraft are found in terms of the Hamiltonian; that is,

$$\mathcal{H}=\min_{\omega_1}[-V_{H_1}\omega_1-(C_1V_{v_1}/g)\omega_1^2]+\max_{\omega_2}[-V_{H_2}\omega_2-(C_2V_{v_2}/g)\omega_2^2]+f(v_1,v_2) \tag{19}$$

where

$$f(v_1,v_2)=V_x\dot x+V_y\dot y+V_{v_1}g(A_1-B_1v_1^2-C_1/v_1^2)-V_{v_2}g(A_2-B_2v_2^2-C_2/v_2^2) \tag{20}$$

To these conditions must be added the maximum turn-rate constraints implied by the sketch of Fig. 2. That is, at velocities between $v_{\min}$ and v_c,

$$|\omega|\le\omega_{\max}=g(k^2v^2-v^{-2})^{\frac{1}{2}} \tag{21}$$

where

$$k=\rho SC_{L_{\max}}/2W$$

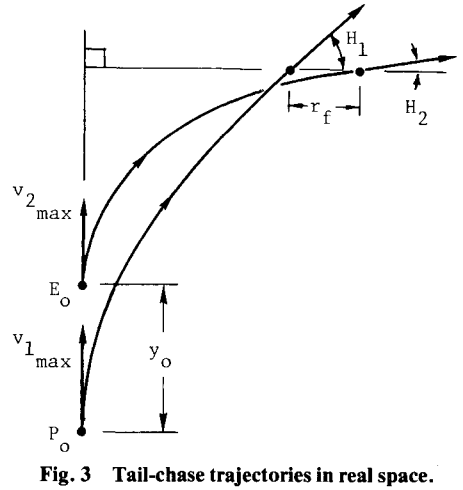

Fig. 3 Tail-chase trajectories in real space.

§It has recently come to the authors' attention that a related study has been carried out by Prasad et al.[8]

Table 1 Parameters for example 1 ($h=0$)

	T^*10^{-3}, kg	W^*10^{-3}, kg	S, m^2	n, g's	A	B^*10^6, s^2/m^2	C^*10^{-3}, m^2/s^2	v_{max}, m/s
Pursuer	15	15	40	5	1.0	6.25	2.10	397
Evader	8.5	10	50	7	0.85	9.37	0.64	300

When the speed is higher than the corner velocity, the maximum turn rate depends upon the structural limit or load factor,

$$|\omega| \le \omega_{max} = g(n^2-1)^{1/2}/v \tag{22}$$

where n is the maximum number of g's in the direction of the inclined lift vector; i.e., $n=\sec\phi$. A typical trajectory pair is shown in Fig. 3.

Method of Solution

In physical terms, the problem solution first requires the determination of the initial range y_0 at which the evader and the faster pursuer break from the constant-speed rectilinear tail-chase geometry. That is, if the evader breaks too soon, at a range greater than y_0, the pursuer knows beforehand in which direction to lead the evader, and the final range will be less than the optimal value. On the other hand, if the evader breaks when the range is less than y_0, the time to minimum range is less, and the evader cannot cross as far ahead of the pursuer; i.e., the final range is again less than the optimal value. The curved trajectories (right or left, at the evader's option) involve time-varying turn rates and speeds, and they end when the range is a minimum. This terminal range is being optimized and is, therefore, initially unknown.

The terminal geometric condition occurs when the radial velocities are equal, as implied by Eq. (12). With our special choice of reference direction, so that $H_1(t_f)=\theta(t_f)$, the stop condition of Eq. (12) reduces to

$$\dot{x}(t_f) = v_2\cos H_2 - v_1\cos H_1 = 0 \tag{23}$$

The six-state optimization problem (with $V_x=1$ and $V_y=0$) is then equivalent to a *reduced* problem with only four states (H_1, H_2, v_1, v_2) and the performance criterion

$$J = \min_{\omega_1}\max_{\omega_2}\int_0^{t_f}(v_2\cos H_2 - v_1\cos H_1)\,dt \tag{24}$$

This criterion is subject to the differential equations on the headings and velocities as given by Eqs. (3-5), where both initial headings are equal to 90 deg, and both initial velocities are maximum. The four terminal adjoints vanish, because the terminal range criterion is not a function of the four reduced states (H_1, H_2, v_1, v_2).

In addition, the initial range is determined by $y(0)=y_0=V_{H_1}(0)+V_{H_2}(0)$, which follows from Eqs. (2) and (15), together with the fact that all of these variables (y, V_{H_1}, and V_{H_2}) vanish at the time of minimum range.

The reduced optimization problem is solved numerically using a differential dynamic programming (DDP) computational procedure. This procedure is initiated by assuming some reasonable control histories, $\bar{\omega}_i(t)$ ($i=1,2$), integrating forward until some time t_f satisfying Eq. (23). The time variations of the velocities and headings (v_i, H_i) are stored, together with those of the controls (ω_i). These state and control variations are then input to the backward integration of the adjoint equations (15-17) and of the equation

$$\dot{a}_i = (\omega_i^* - \bar{\omega}_i)[V_{H_i} + (\omega_i^* + \bar{\omega}_i)V_{v_i}C_i/g] \tag{25}$$

where

$$\omega_1^* = \frac{D_1\bar{\omega}_1 + V_{H_1}}{D_1 - 2C_1V_{v_1}/g} \qquad \omega_2^* = \frac{D_2\bar{\omega}_2 - V_{H_2}}{D_2 + 2C_2V_{v_2}/g} \tag{26}$$

and where ω_i^* is to be replaced by $\omega_{max}(v_i)$ in case ω_i^* exceeds this value. Next, $\bar{\omega}_i$ is replaced by $\omega_i^*(t)$ and the whole procedure is iterated.

Equation (25) is derived by consideration of the change in performance function resulting from small changes in control of both pursuer and evader; i.e.,

$$\Delta J \simeq \int_0^{t_f}[\mathcal{H}(\omega^*) - \mathcal{H}(\bar{\omega})]\,dt$$

or

$$\Delta J = -\int_0^{t_f}[\dot{a}_1(t) + \dot{a}_2(t)]\,dt = a_1(0) + a_2(0) \tag{27}$$

A large value of D_i reduces the change $\omega_i^* - \bar{\omega}_i$. A very small value of D_i is equivalent to maximization of the Hamiltonian with respect to ω_i. Note that $-V_{v_1}$ and V_{v_2} are clearly positive, because V_{v_i} is the sensitivity of miss-distance to v_i. Thus, if v_1 is greater, this miss-distance decreases, while if v_2 is greater, it increases.

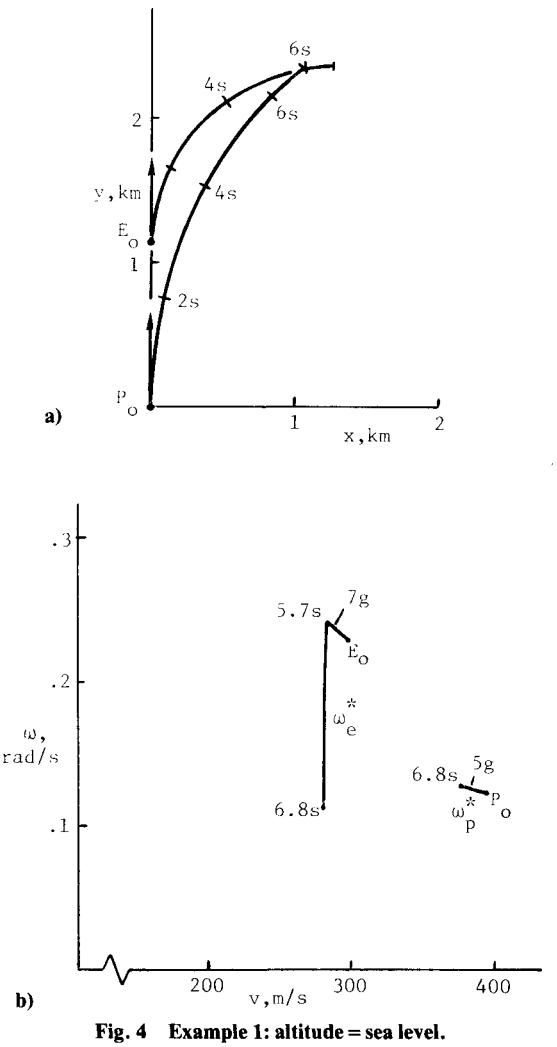

Fig. 4 Example 1: altitude = sea level.

Table 2 Parameters for example 2 ($h=6.6$ km)

	T^*10^{-3}, kg	W^*10^{-3}, kg	n, g's	A	B^*10^6, s^2/m^2	C^*10^{-3}, m^2/s^2	v_{max}, m/s
Pursuer	7.5	15	5	0.5	3.15	4.17	387
Evader	4.25	10	7	0.425	4.72	1.27	295

The change $r_f - \bar{r}_f$ in the payoff, where

$$r_f = \int_0^{t_f} (v_2 \cos H_2 - v_1 \cos H_1)\, dt$$

is compared with $\Delta J = a_1(0) + a_2(0)$. If the correction in the range $r_f - \bar{r}_f$ differs greatly from ΔJ, the weighting parameters D_1 and D_2 are increased during an iteration according to rules given in Refs. 9 and 10.

The last forward integration can include the relative position states (x,y), where $x(0)=0$ and the initial range is $y(0) = V_{H_1}(0) + V_{H_2}(0)$.

Numerical Examples

Example 1

The pursuer and evader are flying at sea level and the parameters are as given in Table 1, where it is noted that the pursuer is less maneuverable (n), but has a higher thrust-to-weight ratio (A). The zero-lift drag coefficients are 0.045 and 0.030, respectively, for P and E, while the induced factors k_D are 0.35 and 0.20. The optimal trajectories are shown in Fig. 4a, while the velocity and turn-rate variations are shown in Fig. 4b. Both aircraft speeds and maximum turn rates are nearly constant, varying by less than 7% during the turn maneuvers. P turns at 5 g's during the entire chase, while E's turn rate is being sharply reduced at the time of minimum range.

The initial and final ranges are $y_0 = 1064$ m and $r_f = 210$ m while the corresponding figures for the constant-speed model[5] are 1155 and 235 m, respectively.¶ These latter figures have been derived using the maximum turn rate which corresponds to cruise velocity for both P and E according to Eq. (21). Both ranges are about 10% less than the constant-speed estimates.

Example 2a

In this modification to the first example problem, the altitude is taken at 6.6 km, where the air density is half its sea-level value and where the maximum thrusts of both aircraft are assumed to be reduced by this same factor. The parameters C_{D_0} and k_D are the same as in example 1. The parameters for the two aircraft are as shown in Table 2, and the corresponding optimal trajectories yield initial and final ranges equal to $y_0 = 903$ m and $r_f = 175$ m as shown in Fig. 5a. These can be compared with the constant-speed values of $y_0 = 1097$ m and $r_f = 228$ m (Ref. 5), and in this case the variable speed values are about 20% less than the constant speed estimates.

The time variations of both speeds and turn rates are shown in Fig. 5b, and it is noted that the evader's turn rate is less than maximum for more than 2 s of the 6.3 s chase. Again, however, the pursuer turns at 5 g during the entire chase.

Example 2b

When the induced-drag factor of the pursuer is varied from $k_D = 0.35$ to other adjacent values, the final range varies monotonically. That is, smaller values of k_D correspond to smaller speed changes in the pursuer's 5 g turn, and to smaller final ranges. As shown in Fig. 6, the variation is more pronounced for higher values of the induced drag. This figure also shows the miss-distance for the constant speed model, in which $k_D = 0$ for both P and E. For this numerical comparison, the parameter B_1 has been adjusted in order to maintain constant the pursuer's maximum velocity.

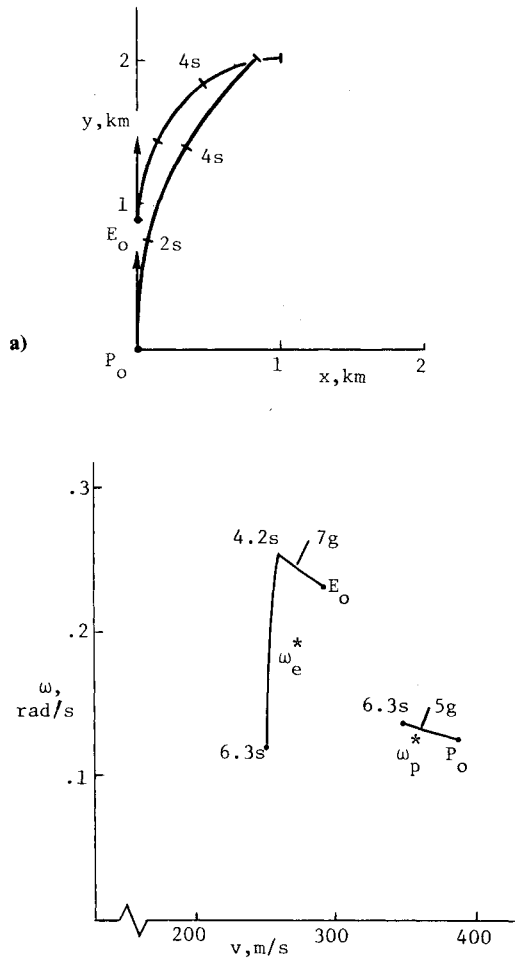

Fig. 5 Example 2: altitude = 6.6 km.

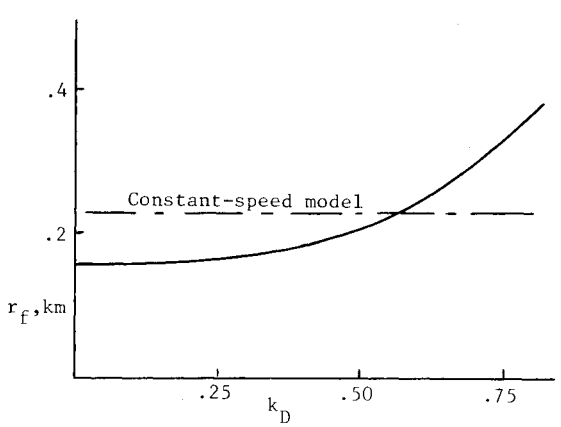

Fig. 6 Optimal miss variation with pursuer's induced drag.

¶In region I of that reference, $y_0 = v_2(1/\omega_1 - 1/\omega_2)$.

Example 3

When the evader's maximum normal acceleration is increased from 7 to 10 g, the terminal miss, of course, increases. The corresponding trajectories and controls at an altitude of 6.6 km are shown in Fig. 7. The initial speeds are as in the previous example, but the optimal initial range, at which E breaks to right or left, is increased to 1595 m, and the final range is 458 m. The parameters for Example 3 are shown in Table 3.

The optimal time variation of E's turn rate is as shown by the solid line in Fig. 7b, and it is noted that maximum turn rate (at 10 g) is optimal for only 1.6 s of the 7.5 s turn maneuver. If E turns at this maximum turn rate until he has turned through 90 deg, the effect is to decrease his velocity considerably and to decrease the miss-distance to $r_f = 407$ m. This nonoptimal control maneuver is initiated by E at the optimal range of 1573 m, and is represented by the dashed curves in Fig. 7. The trajectory of P is slightly shortened, but is otherwise independent of E's maneuver strategy.

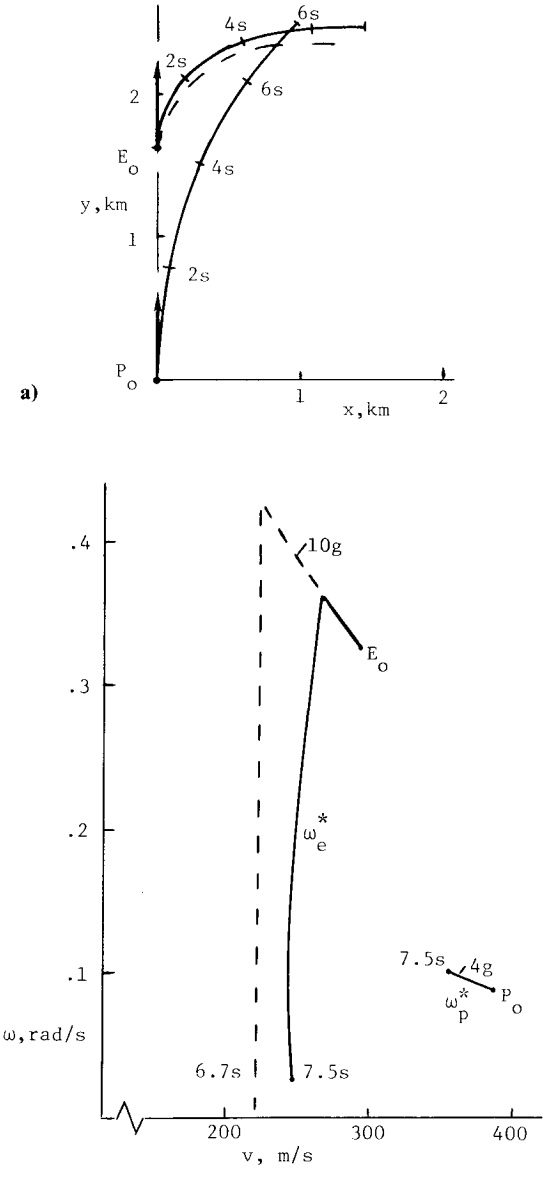

Fig. 7 Example 3: altitude = 6.6 km.

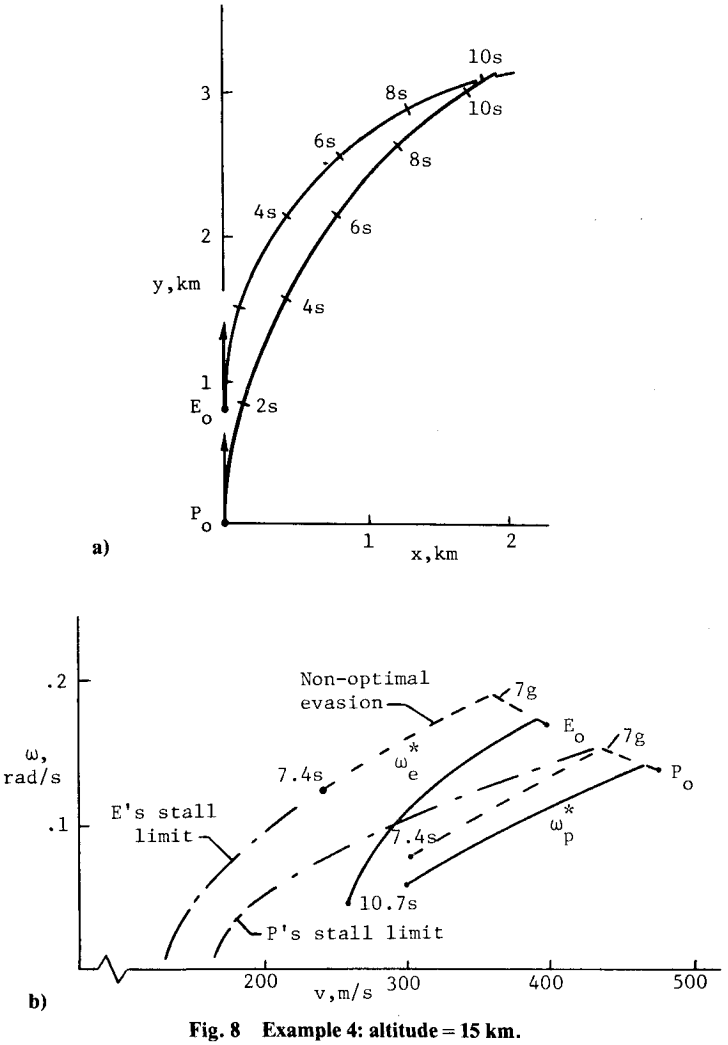

Fig. 8 Example 4: altitude = 15 km.

Table 3 Parameters for example 3 (h = 6.6 km)

	T^*10^{-3}, kg	W^*10^{-3}, kg	n, g's	A	B^*10^6, s^2/m^2	C^*10^{-3}, m^2/s^2	v_{max}, m/s
Pursuer	7.5	15	5	0.5	3.15	4.17	387
Evader	4.2	10	10	0.425	4.72	1.27	295

Table 4 Parameters for example 4 (h = 15 km)

	T^*10^{-3}, kg	W^*10^{-3}, kg	S, m^2	n, g's	A	B^*10^6, s^2/m^2	C^*10^{-3}, m^2/s^2	v_{max}, m/s
Pursuer	4.25	15	40	7	0.283	0.876	19.0	478
Evader	2.75	10	40	7	0.275	1.38	8.86	398

Example 4

When the tail chase occurs at the very high altitude of 15 km (49,200 ft), and the lateral accelerations of both pursuer and evader are equal to 7 g, both trajectories take place across the corner velocity of Fig. 2. In the present case, the parameters and initial speeds are as given in Table 4.

The optimal initial and final ranges are 792 and 82 m, respectively, and the variation of turn rates and velocities lead to the trajectories shown in Figs. 8a and 8b.

It may be noted that neither pursuer nor evader has turned through 90 deg at minimum range, and that neither turns at maximum turn rate for more than a small fraction of the total maneuver time. Nevertheless, both speeds are reduced considerably from their initial values, during the 10.7-s maneuvers shown in Fig. 8a. The corresponding variations in speed and turn rate are shown as the solid lines labeled (ω_p^*, ω_e^*) in Fig. 8b. The constant-speed model of Ref. 5 predicts zero miss-distance, and is in error principally because the speeds actually drop by about 35% during the turn maneuvers. For such high-altitude encounters, the constant-speed model is very poor.

If the evader instead always turns at maximum turn rate and optimizes the range at which his hard-turn maneuver begins, the pursuer's best strategy differs. In this case, the initial and final ranges are 584 and 56 m, respectively. As shown by the dashed lines in Fig. 8b, the pursuer also turns harder, but for a shorter time, and minimum range occurs at 7.4 s.

Conclusions

A variable-speed aerial combat model has been studied using an iterative numerical procedure to develop optimal differential-game solutions in which the terminal range is optimized. The nonlinear aspects of the problem have been treated using a first-order numerical differential dynamic programming method. The pursuit-evasion differential game encourages both high turn rates and high speeds, which cannot be exploited simultaneously. A typical solution requires an initial high turn rate by both aircraft when the velocities fall rapidly, followed by slower turns when the velocity may begin to increase again for either or both aircraft.

Within the limitations of the coplanar dynamic model used, the tail-chase initial condition is optimal from the evader's point of view, because any other initial geometry allows the pursuer to *lead* the evader optimally, which would yield a smaller final range. This would not necessarily be the case if both aircraft could take the role of pursuer.

A more general and realistic model of the combat encounter could include the Mach number variation of both drag coefficient and thrust. Such extensions to the present results could include parameter-sensitivity analysis to determine the variational effects of the coefficients and constraints in the velocity equations. Further generalization could allow full three-dimensional motion of both aircraft, and could determine the applicability of Immelmann and Lufbery turns to the tail-chase initial geometry, using the coplanar results as an initial approximation. A gimballed thrust nozzle is another potential generalization of particular interest when the induced drag is high.

References

[1] Isaacs, R., *Differential Games,* Wiley, New York, 1965, pp. 202, 237-244.

[2] Merz, A.W., "The Game of Two Identical Cars," *Multicriteria Decision Making and Differential Games,* edited by G. Leitmann, Plenum Press, New York, 1976, pp. 421-442.

[3] Peng, W.Y. and Vincent, T.L., "Some Aspects of Aerial Combat," *AIAA Journal,* Vol. 13, Jan. 1975, pp. 7-11.

[4] Vincent, T.L., "Avoidance of Guided Projectiles," *The Theory and Application of Differential Games,* edited by J.D. Grote, D. Reidel Publishing Co., Dordrecht, Holland, 1975, pp. 267-279.

[5] Breakwell, J.V. and Merz, A.W., "Minimum Required Capture Radius in a Coplanar Model of the Aerial Combat Problem," *AIAA Journal,* Vol. 15, Aug. 1977, pp. 1089-1094.

[6] Olsder, G.J. and Breakwell, J.V., "Role Determination in an Aerial Dogfight," *International Journal of Game Theory,* Vol. 3, 1974, pp. 47-66.

[7] Merz, A.W. and Hague, D.S., "Coplanar Tail Chase Aerial Combat as a Differential Game," *AIAA Journal,* Vol. 15, Oct. 1977, pp. 1419-1423.

[8] Prasad, U.R., Rajan, N., and Rao, N.J., "Planar Pursuit-Evasion with Variable Speeds," Parts I and II, *Journal of Optimization Theory and Application,* Vol. 22, March 1981.

[9] Järmark, B.S.A., "On Convergence Control in Differential Dynamic Programming Applied to Realistic Aircraft and Differential Game Problems," *Proceedings of the 1977 IEEE Conference on Decision and Control,* Dec. 1977, pp. 471-479.

[10] Järmark, B.S.A., "Differential Dynamic Programming Techniques in Differential Games," *Control and Dynamic Systems,* edited by C.T. Leondes, Vol. 17, Academic Press, New York, 1980.